

# Scalar mesons in the chiral theory with quark degrees of freedom

M.S. Lukashov and Yu.A. Simonov  
 Institute for Theoretical and Experimental Physics,  
 NRC “Kurchatov Institute”  
 Moscow, 117218 Russia

May 19, 2020\*

## Abstract

The Chiral Confining Lagrangian, based on the chiral theory with quark degrees of freedom, is used to study the spectroscopy of scalar mesons. The formalism does not contain arbitrary fitting parameters and takes into account infinite number of transitions from meson-meson to quark-antiquark states. Starting from known  $q\bar{q}$  poles the transition coefficients ensure the strong shift of the poles for the  $\pi\pi$  and much smaller shift for the  $K\bar{K}$  systems. The resulting amplitudes  $f_{\pi\pi}$  and  $f_{K\bar{K}}$  are calculated in terms of the  $q\bar{q}$  and the free meson Green’s functions. With the account of the  $\pi\pi/K\bar{K}$  channel coupling one obtains two resonances: a wide resonance  $E_1$  in the range 500-700 MeV and narrow  $E_2$  near 1 GeV, which can be associated with  $f_0(500)$  and  $f_0(980)$ . A similar analysis, applied to the  $I = 1$  channel, shows that in this case two very close poles in different sheets appear near  $E = 980$  MeV, which can be associated with the  $a_0(980)$  resonance. The obtained  $\pi\pi$  interaction amplitudes,  $\text{Re } f_{\pi\pi}(E)$  and  $\text{Im } f_{\pi\pi}(E)$  are compared with the known data.

## 1 Introduction

Scalar mesons are in the center of experimental and theoretical interests for a long time (see summary of experimental data in Ref. [1] and a large amount of information about the scalars in the reviews [2, 3, 4, 5, 6, 7], and recent comprehensive analysis in [8, 9]). The theoretical explanation of the scalar spectrum

---

\*v5 for arXiv (accepted to PRD)

has faced difficulties and required the development of different approaches, like the tetraquark model [10], the molecular approach [11], and the QCD sum rules [12], as well as lattice calculations [13] (see recent study in [14]).

It is clear, that in QCD any meson state can be represented as a series  $M = c_1 (q\bar{q}) + c_2 (q\bar{q})^2 + \dots$ , where higher terms can be transformed into mesons as  $(q\bar{q})^n = m_1 m_2 \dots$ . Mesons with nonzero  $q\bar{q}$  component can be called standard, while those with  $c_1 = 0$  –nonstandard or exotic. For standard mesons the original  $q\bar{q}$  pole can be shifted due to  $q\bar{q}$ - $mm$ - $q\bar{q}$  interaction, as it is known from comparison with experiment. However, the  $m_1 m_2$  interaction can be strong enough to produce bound states and resonances as it happens in nuclear physics. In what follows we shall study scalar resonances in QCD, starting from the standard  $q\bar{q}$  component and describing the physical scalar resonance as the result of multiple  $q\bar{q}$ - $m_1 m_2$  transitions. In principle this approach is not new and has been worked out in [15, 16, 17, 18, 19, 20, 21, 22], where transitions have been properly parametrized. On another hand, one can have additional poles due to  $m_1 m_2$  interaction. The latter can be introduced in the framework of the meson-meson interaction in the unitarized chiral perturbation theory (also on top of quark model resonances) [23, 24, 25, 26, 27, 28, 29], and here e.g.  $f_0(500)$  becomes heavier and more narrow, when  $mm$  interaction is suppressed [24, 25]. For the results of the unitarized chiral perturbation theory and inclusion of NLO terms see [27, 28] and the review paper [8]. With all that one can stress that the Chiral Perturbation Theory is not necessary for obtaining these results and one can use the dispersive methods and the data to obtain a good explanation of  $f_0(500)$  and other resonances, see e.g. [30, 31, 32].

As it is, the situation with the scalar mesons, and first of all, with lowest scalar mesons, is still unclear and calls for new ideas. As one can see in [1], Table 2, the conventional opinion considers the resonances  $a_0(1450)$  and  $f_0(1370)$  as the lowest  ${}^3P_0$  states for  $I = 1, 0$  respectively. On the other hand, numerous calculations of the lowest  ${}^3P_0$   $q\bar{q}$  states with realistic  $q\bar{q}$  interaction, including spin-dependent forces refer to  $a_0(980)$  ( $f_0(980)$ ) as the lowest  ${}^3P_0$  states, see e.g. [33], while  $a_0(1450)$  might be only connected to the first excited state.

There is no general consensus on the lowest states ( $f_0(500)$ ,  $f_0(980)$ ,  $a_0(980)$ ) in the modern approaches, including the attempts to derive these states in the molecular or tetraquark approaches. Unfortunately also in this latter approach a recent lattice calculation [34] of the  $a_0(980)$  state with account of tetraquark ( $q^2\bar{q}^2$ ) contribution does not show any explicit influence of the latter on the lowest states, thus calling for a new dynamics as a possible source of  $f_0(500)$ ,  $f_0(980)$ ,  $a_0(980)$ .

It is the purpose of the present paper to suggest a new approach to the

solution of this problem and to demonstrate a new quark-chiral dynamics, which might explain the origin of the lowest scalar states. The essence of the method is as follows.

The main problem of the most part of approaches to the scalar mesons from our point of view is the imbalance in the treatment of quark and meson d.o.f. In reality meson-meson ( $\varphi\varphi$ , e.g.  $\pi\pi, K\bar{K}$ ) and  $q\bar{q}$  d.o.f. have to be considered on equal footing, since both can transform into each other at any moment of time. Moreover, the  $q\bar{q}$  poles are accurately predicted at the proper places by the relativistic QCD theory with scalar confinement and gluon exchanges [35, 36, 37] in all channels [38, 39] and in many cases they are observed in experiment shifted by 50-80 MeV or less.

Therefore, the  $q\bar{q}$  poles should be seen in experiment as the  $\varphi\varphi$  resonances, shifted or not shifted. On another hand one may think of some (or all)  $\varphi\varphi$  resonances as produced by the  $\varphi\varphi$  interaction, e.g. by the unitarized chiral dynamics, where  $q\bar{q}$  dynamics does not play any role. Instead, we consider the coupled  $\varphi\varphi - q\bar{q}$  system with the proper  $q\bar{q}$  dynamics and the transition dynamics of  $q\bar{q}$  into  $\varphi\varphi$  system, first neglecting the  $\varphi\varphi$  interaction and introducing it at the next stage.

Therefore, one needs the formalism of the two-channel  $q\bar{q}, \varphi\varphi$  Green's functions, which takes into account any number of  $q\bar{q} - \varphi\varphi$ , and  $\varphi\varphi - q\bar{q}$  transitions. In the case of scalar mesons this type of formalism was already exploited in [15, 16, 17, 18, 19, 20, 21, 22]. In the case of the heavy quarks this formalism, considering  $Q\bar{Q}$  and  $(Q\bar{q}) + (\bar{Q}q)$  channels nonrelativistically, was suggested in [40], and was called the Cornell formalism. It was used in [41] to discover the nature of the resonance  $X(3872)$ , with  $c\bar{c} 2^3P_1$  state transforming into  $DD^*$ , via string breaking mechanism, which finally brings it to the  $D_0D_0^*$  threshold at 3872 MeV [42].

We shall generalize the Cornell formalism, making it relativistic and multi-channel, when one  $q\bar{q}$  state can transform into several  $\varphi\varphi$  states, and we shall neglect at the first stage the interaction between white  $\varphi\varphi$  mesons.

The full analysis of the scalars requires the multichannel approach to the problem, where several quark-antiquark ( $q\bar{q}$ ) channels are present together with two or more Nambu-Goldstone boson channels ( $(\varphi\varphi)$  channels). Therefore, complete formulation requires the knowledge of 1) the Green's functions both in  $q\bar{q}$  and  $\varphi\varphi$  channels; 2) the transition matrix elements between the channels. Without explicit knowledge of these entries one faces the multi-parameter and multi-channel situation with hardly possible informative output.

The treatment of the first point – the spectral representation of the  $q\bar{q}$  Green's function with accurate calculation of one-channel  $q\bar{q}$  poles and cou-

plings, can be done in the framework of the Field Correlator Method (FCM) (see [36, 37] for reviews and [38] for recent calculations in different channels). The  $\varphi\varphi$  Green's function in the initial one-channel set-up will be studied here, assuming that it can be replaced by the free two-body propagators and possible resonances exist only due to channel coupling, in particular, with the  $q\bar{q}$  channels, and here the problem 2) becomes a basic point in a new approach.

Indeed, in the heavy quarkonia the channel coupling with the heavy mesons is described by the string breaking mechanism (sometimes with emission of pions), which brings in the resonance shift of  $O(50 - 100)$  MeV. In the case of scalar mesons the  $\varphi\varphi$  channel contains chiral mesons and the transition process from  $\varphi\varphi$  to  $q\bar{q}$  and back requires a different approach.

During the last 15 years one of the authors has succeeded to derive the Chiral Confining Lagrangian (CCL) - the powerful tool for the study of chiral effects in connection with quark d.o.f. [43, 44]. The latter is actually an extension of the standard Chiral Lagrangian, which contains both the quark and chiral d.o.f. and tends to the standard Chiral Lagrangian [45] when quark d.o.f. are neglected; all coefficients of CCL are easily calculated, as it was done in [44] in the order of  $p^4$ . Moreover, the basic factors, like  $f_\pi, f_K$ , are calculated within this method [46]. The only basic parameter,  $M(\lambda) = \sigma\lambda$ , which appears due to confinement, is a fixed quantity, defined by the transition radius  $\lambda$ . The latter is calculated at the stationary point and is expressed via string tension  $\sigma$  and masses [56] and as a result our method does not contain any fitting parameters. In this way the CCL method allows to find analytically all entries 1) and 2), while the scalar decay constants  $f_s$  are calculated in the same way as  $f_\pi, f_K$  within the FCM, using the spectral representation of the Green's function.

In principle, our method gives a possibility of treating any process with multiple  $q\bar{q}$  and any number of  $\varphi\varphi$  channels; the advantage of using the CCL is that for scalar mesons all transition coefficients are known. In the case of a single  $\varphi\varphi$  and a single  $q\bar{q}$  channel our results can be written in the form, comprising the Breit-Wigner resonance, similarly to results in Refs. [15, 16, 17, 18, 19, 20, 21, 22]. However, in the case of multiple  $\varphi\varphi$  channels more complicated expressions are obtained, using the  $K$ -matrix approach.

As will be seen, the essence of our approach is the summation of the infinite re-scattering series with multiple transitions between  $\varphi\varphi$  and  $q\bar{q}$  states, which yields several poles. In this way we obtain two poles in the regions of  $f_0(500)$  and  $f_0(980)$ , which finally obtain realistic positions when  $\varphi\varphi$  interaction is taken into account.

The paper is organized as follows. In the next section the general structure of the coupled-channel Green's function for a scalar meson is derived from CCL,

and we define basic quantities 1), 2) in terms of known standard coefficients. In section 3 we discuss the  $q\bar{q}$  Green's functions in the spectral form and the free  $\varphi\varphi$  Green's functions and use the decay constants and the pole masses from the known confining, gluon exchange and spin-dependent interaction. Note, that this calculation does not use any parameters, beyond the string tension, the current quark masses,  $\Lambda_{QCD}$ , and  $M(\lambda)$ . In section 4 we discuss the resulting  $\varphi\varphi|q\bar{q}$  Green's function and find the physical  $\varphi\varphi$  amplitudes ( $\pi\pi$  and  $K\bar{K}$ ), containing two resonances, which can be associated with  $f_0(500)$  and  $f_0(980)$ . In section 5 these results are augmented by the calculation of the real and imaginary parts of the  $\pi\pi$  amplitude, which are qualitatively similar to the results, obtained from theory and experiment at least for  $E > 500$  MeV. We demonstrate in Fig. 5 and 6 that by a proper modification of the  $\pi\pi$  Green's function one is able to reproduce these data, and the resulting  $\pi\pi$  resonance is made closer to the experiment. We also show that in the case of the isospin  $I = 1$  our method gives a different picture of two nearby poles within 50 MeV in different sheets for  $a_0(980)$ . Section 6 contains discussion and an outlook.

## 2 Coupled channel equations for the scalars from the Chiral Confining Lagrangian

In what follows we are using the Chiral Confining Lagrangian (CCL) [43, 44] with the scalar external currents  $s_0(x)$  and  $s_a(x)\lambda^a \equiv \hat{s}$  for isospin  $I = 0$  and  $I = 1$ , respectively.

$$L_{CCL} = -N_c \text{tr} \log(\hat{\partial} + \hat{m} + s_0 + \hat{s} + M\hat{U}), \quad (1)$$

In Eq. (1)  $\hat{\partial}$  implies  $\frac{\partial}{\partial x_\mu} \gamma_\mu$  and  $\hat{U}$  is the standard chiral operator,

$$\hat{U} = \exp(i\gamma_5 \hat{\varphi}), \quad \hat{\varphi} = \frac{\varphi_a \lambda_a}{f_a}, \quad (2)$$

$$\hat{\varphi} = \sqrt{2} \begin{pmatrix} \frac{1}{f_\pi} \left( \frac{\eta}{\sqrt{6}} + \frac{\pi^0}{\sqrt{2}} \right), & \frac{\pi^+}{f_\pi}, & \frac{K^+}{f_K} \\ \frac{\pi^-}{f_\pi}, & \left( \frac{\eta}{\sqrt{6}} - \frac{\pi^0}{\sqrt{2}} \right) \frac{1}{f_\pi}, & \frac{K^0}{f_{K^0}} \\ \frac{K^-}{f_K}, & \frac{\bar{K}^0}{f_{K^0}}, & -\frac{2\eta}{\sqrt{6}f_\pi} \end{pmatrix} \quad (3)$$

In (2)  $\lambda_a$  are the Gell-Mann matrices,  $\text{tr} \lambda_a \lambda_b = 2\delta_{ab}$ . One can consider CCL in (1) as a generating functional for different vertices and Green's functions.

Indeed, omitting  $s_0$  and  $s$ , one can expand, as in [43, 44] in powers of  $\hat{U}^+ \Lambda (\hat{\partial} + \hat{m})(\hat{U} - 1) = \eta$  which dimensionless and yields an expansion in  $S \hat{\partial} \hat{\phi}$ , which is an expansion in quark loops (here  $S = i\Lambda$  is the quark propagator) times derivative of chiral field  $\phi$  – this gives  $O(p^4)$  terms in good agreement with standard calculations, and the same expansion yields standard GMOR relation – see [44] for details. In our case we need another expansion in powers of dimensionless quantity,  $\Lambda M(U - 1)$ , which is done as follows.

Using the scalar currents  $s_0, \hat{s}$ , one can generate the scalar Green's functions  $G_{q\bar{q}}^s, G_{\varphi\varphi}^s$ .

$$\begin{aligned} L_{CCL} &= -N_c \text{tr} \log(\Lambda^{-1} + s_0 + \hat{s} + M(\hat{U} - 1)) = -N_c \text{tr} \log \Lambda^{-1} (1 + \Lambda(s_0 + \hat{s} + M(\hat{U} - 1))) = \\ &= \frac{N_c}{2} \text{tr} \{ (\Lambda(s_0 + \hat{s}) \Lambda(s_0 + \hat{s})) + \dots \} = \frac{N_c}{2} (G_{q\bar{q}}^{s_0} + G_{q\bar{q}}^{\hat{s}}) + \dots \end{aligned} \quad (4)$$

Here  $\Lambda = \frac{1}{\hat{\partial} + \hat{m} + M}$ . The corresponding diagram is shown in Fig.1 One can write  $G_q^s(x, y) = \text{tr} (\bar{s}(x) g_{q\bar{q}}(x, y) s(y))$ , where  $g_{q\bar{q}}$  will be used later.

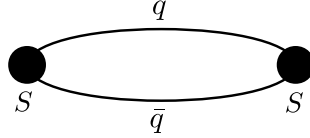


Figure 1: The scalar  $q\bar{q}$  Green's function  $G_{q\bar{q}}$ .

On the other hand, expanding the CCL (4) in powers of  $\Lambda M(\hat{U} - 1) \equiv \xi$ , one obtains another term in the second order in  $\xi$ ,

$$\Delta L = -N_c \text{tr} \Lambda s \Lambda M \frac{\hat{\varphi}^2}{2}, \quad s = s_0 + \hat{s}; \quad (5)$$

which corresponds to the diagram of Fig. 2. Note, that in this way we can obtain the vertices for all chiral decays of any  $q\bar{q}$  state, e.g.  $a_2$  meson decaying into  $3\pi$  etc.

In (1) the confining kernel  $M(r)$  enters either inside the propagating  $q\bar{q}$  system, in which case it is equal to the confining potential,  $M(r) = \sigma r$ , or else it appears at the vertex of the  $q\bar{q}$  Green's function, connecting it to the  $\varphi\varphi$  Green's function. In this case the vertex  $M(r)$  is taken at the effective distance  $\lambda$ ,  $M = M(\lambda) = \sigma\lambda$ . One can consider this distance  $\lambda$  as the spatial width of the transition vertex, connecting  $\varphi\varphi$  and  $q\bar{q}$  channels, see Fig.3. In the case

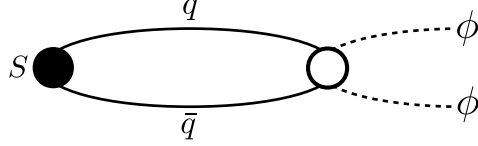


Figure 2: The scalar  $q\bar{q}$  Green's function with the emission of the chiral mesons.

of one chiral meson we take it approximately equal to the correlation length in the confining vacuum,  $\lambda \approx 0.2$  fm, yielding  $M(\lambda) = 0.15$  GeV. As a check of this approximation, this value was used to calculate  $f_\pi$  and  $f_K$  [46] in good agreement with experimental and lattice data and therefore we shall consider  $\lambda$  in the range  $(0.2 \div 0.3)$  fm (or  $1 \div 1.5$  GeV $^{-1}$ ) in what follows. This factor  $M(\lambda)$  appears to be the only parameter of our quark-chiral approach in (1) in addition to the quark masses  $m_q$  and string tension  $\sigma$ .

From (5) one can find the basic quantity, which will be used below, – the transition element  $V_{q\bar{q}\varphi\varphi}$  which joins the  $q\bar{q}$  Green's function  $g_{q\bar{q}}$  and the  $\varphi\varphi$  Green's function  $g_{\varphi\varphi}$ , see Fig.4 and its definition below. At this point it is important to understand which kind of the  $q\bar{q}$  Green's function is needed to join it with the  $g_{\varphi\varphi}$ , i.e. to annihilate at one vertex  $q\bar{q}$  and create at this vertex two mesons  $\varphi\varphi$ . One clearly needs  $g_{q\bar{q}}(x, y) \sim (S_q(x, y)S_{\bar{q}}(x, y))$ , where  $S_q(x, y)$  is the quark Green's function, but with the definite total momentum, i.e.  $g_{q\bar{q}}(P) = \int d^4(x-y)e^{iP(x-y)} \text{tr}(S_q(x, y)S_{\bar{q}}(x, y))$ ; originally  $g_{q\bar{q}}(x, y)$  should be connected with  $g_{\varphi\varphi}$  at the same point  $x$  or  $y$  and finally with  $g_{\varphi\varphi}(P)$ . However,  $g_{\varphi\varphi}(P)$  is divergent in its real part, which implies that the transition from  $q\bar{q}$  to  $\varphi\varphi$  occurs not in one point, but at some distance between  $q$  and  $\bar{q}$ , namely, at the same distance between  $\varphi$  and  $\varphi$  which we call  $r_0 \sim \lambda \sim 0.2$  fm – the transition radius, which is shown in Fig.3.

It is important that at this moment the  $M(r)$  becomes  $M(\lambda) = \sigma\lambda \approx 0.15$  GeV, and  $\text{Re } g_{\varphi\varphi}$  should have an initial and final  $\varphi - \varphi$  distance  $\lambda$ . As will be shown below, this transition radius does not change much the  $g_{q\bar{q}}(\lambda)$ , which is anyhow convergent at  $\lambda = 0$ , but the variation of  $\text{Re } g_{\varphi\varphi}(\lambda)$  can be taken into account. In this approximation the total scalar Green's function can be written as

$$G^s = g_{q\bar{q}}^s + g_{q\bar{q}}^s V g_{\varphi\varphi}^s V g_{q\bar{q}}^s + \dots = g_{q\bar{q}}^s \frac{1}{1 - V g_{\varphi\varphi}^s V g_{q\bar{q}}^s} \quad (6)$$

Here  $V \equiv V_{q\bar{q}/\varphi\varphi}$  can be found from (5), see below.

As it is seen from (5), the transition coefficient  $V$  is proportional to  $\frac{M(\lambda)}{f_\varphi^2}$ ,  $\varphi =$

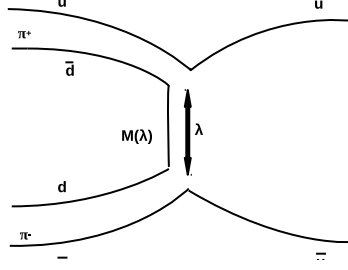


Figure 3: The transition region ( $q\bar{q}|\varphi\varphi$ ) with the spatial distance  $\lambda$  between the constituents.

$\pi$ ,  $K$ , and also to the quark decay constant of the scalar meson  $f_s^{(n)}$ , ( $n = 1, 2, \dots$ ) to be found below.

Finally, to define how  $V$  depends on isotopic indices, one can according to (5), project  $\frac{\hat{\varphi}^2}{2}$  on a given isotopic state with  $I = 0$  or 1.

$$\text{tr} \left( s_0 \frac{\hat{\varphi}^2}{2} \right) = s_0 (a_{11} + a_{22} + a_{33}); \quad (7)$$

$$\begin{aligned} \text{tr} \left( s_i \lambda_i \frac{\hat{\varphi}^2}{2} \right) &= a_{11} \left( s_3 + \frac{1}{\sqrt{3}} s_8 \right) + a_{22} \left( -s_3 + \frac{1}{\sqrt{3}} s_8 \right) + a_{12} (s_1 + i s_2) + \\ &+ a_{21} (s_1 - i s_2) - a_{33} \cdot \frac{2}{\sqrt{3}} s_8 \end{aligned} \quad (8)$$

where  $a_{ik}$  are

$$a_{11} = \frac{1}{f_\pi^2} \left[ \left( \frac{\eta}{\sqrt{6}} + \frac{\pi^0}{\sqrt{2}} \right)^2 + \pi^+ \pi^- \right] + \frac{K^+ K^-}{f_K^2}, \quad (9)$$

$$a_{12} = \frac{2\eta\pi^+}{f_\pi^2 \sqrt{6}} + \frac{K^+ \bar{K}^0}{f_K^2}, \quad a_{21} = \frac{2\eta\pi^-}{f_\pi^2 \sqrt{6}} + \frac{K^0 \bar{K}^-}{f_K^2}, \quad (10)$$

$$a_{22} = \frac{1}{f_\pi^2} \left[ \left( \frac{\eta}{\sqrt{6}} - \frac{\pi^0}{\sqrt{2}} \right)^2 + \pi^+ \pi^- \right] + \frac{K^0 \bar{K}^0}{f_K^2}, \quad (11)$$

$$a_{33} = \frac{K^+ K^- + K^0 \bar{K}^0}{f_K^2} + \frac{2\eta^2}{3 f_\pi^2}. \quad (12)$$



Later we shall neglect the isotopic (SU(3)) dependence of the propagators  $\Lambda$ , apparent in the mass matrices  $\hat{m}$ , and take it in account at the end, since one can write  $g_{q\bar{q}} \equiv g_1 = \begin{pmatrix} g_1(n\bar{n}) & 0 \\ 0 & g_1(s\bar{s}) \end{pmatrix}$ .

### 3 The $q\bar{q}$ Green's functions and the eigenvalues

To calculate the  $q\bar{q}$  Green's functions we shall use the exact relativistic formalism, based on the FCM [35] and essentially exploiting relativistic path integral methods [37, 38, 39, 47, 48]; at the end we shall compare our results with those obtained in other methods.

The  $q\bar{q}$  Green's function  $g_{q\bar{q}}^\Gamma(x, y) \equiv g_1(x, y)$  with the vertex  $\Gamma$ , defining the spin-parity, can be written as

$$g_1(x, y) = \text{tr} \left( \frac{4Y}{(m_1^2 - \hat{D}_1^2)(m_2^2 - \hat{D}_2^2)} \right) \quad (13)$$

where

$$4Y = \text{tr}[\Gamma(m_1 - \hat{D}_1)\Gamma(m_2 - \hat{D}_2)]. \quad (14)$$

Then using the relativistic path integral formalism (see [47, 48, 49] for a review) it can be written in the c.m. system and in the Euclidean time  $T$

$$\int d^3(\mathbf{x} - \mathbf{y})g_1(x, y) = \frac{T}{2\pi} \int_0^\infty \frac{d\omega_1}{\omega_1^{3/2}} \int_0^\infty \frac{d\omega_2}{\omega_2^{3/2}} \langle Y \rangle \langle 0 | e^{-H(\omega_1, \omega_2, \mathbf{P})T} | 0 \rangle. \quad (15)$$

Here the c.m. Hamiltonian  $H(\omega_1, \omega_2, \mathbf{p})$  depends on the virtual energies  $\omega_1, \omega_2$  and includes all instantaneous interactions, including spin and angular momentum dependent,

$$H(\omega_1, \omega_2, \mathbf{p}) = \sum_{i=1,2} \frac{\mathbf{p}^2 + \omega_i^2 + m_i^2}{2\omega_i} + V_0(r) + V_{so} + V_T. \quad (16)$$

Here  $V_0(r) = \sigma r - \frac{4\alpha_V(r)}{3r}$ ,  $V_{so}$  is the spin-orbit interaction and  $V_T$  is the tensor interaction, both in the relativistic form. Neglecting spin terms, one can rewrite the last term in (15) as

$$\langle 0 | e^{H(\omega_1, \omega_2, \mathbf{P})T} | 0 \rangle = \sum_{n=0} \varphi_n^2(0) e^{-M_n(\omega_1, \omega_2)T}, \quad (17)$$

where  $\varphi_n(\mathbf{r})$  is the wave function. On the other hand one has a general relation

$$\int g_1(x, y) d^3(\mathbf{x} - \mathbf{y}) = \sum_n \int d^3(\mathbf{x} - \mathbf{y}) \langle 0 | j_\Gamma | n \rangle \langle n | j_\Gamma | 0 \rangle \times$$

$$e^{i\mathbf{P}(\mathbf{x}-\mathbf{y})-M_n T} \frac{d^3\mathbf{P}}{2M_n(2\pi)^3} = \sum_n \varepsilon_\Gamma \otimes \varepsilon_\Gamma \frac{(M_n f_\Gamma^{(n)})^2}{2M_n} e^{-M_n T} \quad (18)$$

This relation allows to calculate the scalar decay constant  $f_s^{(n)}$ , which is done in Appendix 1.

Note, that using CCL, Eq.(1), one would have in (14)  $m_i + M(\lambda)$  instead of  $m_i$ , which allows obtaining in the PS case ( $\Gamma = \gamma_5$ ) the correct decay constants  $f_\pi, f_K$ , [46], which otherwise would be zero in the zero quark mass limit.

In (15) it is convenient to integrate over  $d\omega_1, d\omega_2$ , using the stationary-point method, and for vanishing quark masses  $m_i = 0$  one obtains the so-called spinless Salpeter equation; if spin-dependent interactions are neglected. In the first approximation one has

$$(2\sqrt{\mathbf{p}^2} + V_0(r))\varphi_{nl}(r) = M_{cog}(nl)\varphi_{nl}(r), \quad (19)$$

where  $M_{cog}$  means the center-of-gravity mass. Later we use only the fundamental parameters:  $\sigma = 0.182(2)$  GeV<sup>2</sup> and  $\Lambda_V(n_f = 3) = 0.465(15)$  GeV, which are well established (see [50] for the definition of  $\Lambda_V$  and an accurate perturbative treatment of scalar mesons), and obtain

$$M_{cog}(1P) = 1259(10) \text{ MeV}, \quad \omega_0(1P) = 499 \text{ MeV}. \quad (20)$$

Doing calculations in the same way as in [37, 38, 39], we give here the resulting mass of the  $1^3P_0$  state with account of the tensor and spin-orbit forces

$$M(1^3P_0) = (1259(10) - 214) \text{ MeV} = 1045(10) \text{ MeV}, \quad (21)$$

which defines the  $q\bar{q}$  initial mass of  $f_0$  and  $a_0$ , taken below, as  $M_1 = 1$  GeV. This mass can be compared with that obtained by other groups, where in [51]  $M(0^{++}) = 1090$  MeV, while in [52]  $M(0^{++}) = 1176$  MeV, and in [53],  $M(0^{++}) = 970$  MeV.

Note, that the first excited state in the  $0^{++}, I = 0$  channel is obtained to be  $M_2 = 1474$  MeV [49] and this state can be associated with the  $a_0(1450)$ .

Finally, we can use (18) to calculate the full Fourier transform of  $g_1(x, y)$  in the Minkowskian time, which yields

$$\tilde{g}_1(P) = \tilde{g}_1(E, \mathbf{P} = 0) = \sum_n \frac{(f_s^{(n)})^2 M_n^2}{M_n^2 - E^2}. \quad (22)$$

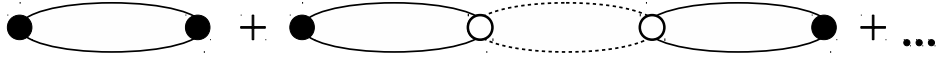


Figure 4: The  $\pi\pi$  interaction amplitude in terms of the  $q\bar{q}$  (solid lines) and  $\pi\pi$  Green's functions (broken lines). The filled and empty circles denote the transition matrix elements  $V_{\pi 1} = V_{1\pi}$ .

This form with the lowest  $n = 1$  will be used below to analyse the scalars  $f_0$ ; it will be shown that the level  $M_1 = 1045$  MeV generates both  $f_0(500)$  and  $f_0(980)$  resonances, connected respectively with the  $\pi\pi$  and  $K\bar{K}$  Green's functions.

We turn to the structure of the meson-meson Green's function, which at first we take as free two body relativistic Green's function of two scalar particles with the total momentum  $\mathbf{P} = 0$  and the total c.m. energy  $E$ . See Appendix 2 for the detailed discussion.

Then in the  $\varphi\varphi$  channel the free Green's function of  $\varphi\varphi$  displaced by a spatial distance  $\lambda$  and averaged over its direction ( $S$ -wave) brings in an additional factor  $f_2(|\mathbf{p}|\lambda)$ :

$$g_2(E) = \int \frac{f_2(|\mathbf{p}|\lambda)d^4p}{(2\pi)^4(p^2 - m_1^2)((P - p)^2 - m_2^2)}, \quad (23)$$

with  $\mathbf{P} = 0$ ;  $P_0 = E$ . Its imaginary part is

$$\text{Im } g_2(E) = \frac{\sqrt{(E^2 - (m_1 + m_2)^2)(E^2 - (m_1 - m_2)^2)}}{16\pi E^2}, \quad (24)$$

One can compare (24) with the cut-off integral, where for equal masses  $m_1 = m_2 = m$  one has for the real part with the cut-off function  $f_1(|\mathbf{p}|\lambda) = \theta(1 - |\mathbf{p}|\lambda)$ ,  $N = 1/\lambda$

$$\text{Re } g_2(E = 2m) = \frac{1}{8\pi^2} \ln \left( \frac{N + \sqrt{N^2 + m^2}}{m} \right). \quad (25)$$

Note, that  $f_2(|\mathbf{p}|\lambda)$  is not a cut-off introduced by hand, as  $f_1(|\mathbf{p}|\lambda)$  which will be used below for comparison. Moreover,  $f_2$  is a part of a physical amplitude, not violating unitarity in the case of spatial distance, and therefore not producing additional singularities. Indeed, one can see this in the explicit form, since  $f_2$  is expanded in even powers of  $\mathbf{p}$ .

In the case of the spatial cut-off  $f_2(|\mathbf{p}|\lambda)$ , when the initial and final distances between  $\varphi\varphi$  are equal to  $\lambda$ , we have  $f_2(x) = \left(\frac{\sin x}{x}\right)^2$ , and the resulting difference between the two real parts with  $f_1$  and  $f_2$  is less than 10% for  $\lambda = (0.5 \div 2)$   $\text{GeV}^{-1}$ .

Note, that the spatial cut-off does not introduce branch points into  $g_2(E)$  and therefore does not spoil unitarity.

## 4 Analytic structure of physical amplitudes

We start with the transition coefficient, which we denote  $k^{(I)}(q\bar{q}|\varphi\varphi)$  and define it in the following way. Using the definition of  $\tilde{g}_1(P)$  (22) and leaving for  $\tilde{g}_1$  only the combination  $\frac{M_n^2}{M_n^2 - E^2}$ , one can associate the transition coefficient with the following combination

$$k^{(I)}(q\bar{q}|\varphi\varphi) = V_{\bar{q}q|\varphi\varphi} V_{\varphi\varphi|q\bar{q}} = (V_{q\bar{q}|\varphi\varphi})^2 = \frac{C_i^2 M^2(\lambda) (f_s^{(n)})^2}{f_\varphi^4}, \quad f_\varphi = f_\pi, f_K. \quad (26)$$

Here the coefficient  $C_i$  can be found from (7 - 12). Introducing notation  $C_i = C_{\text{meson,meson}}^I$  one obtains from (5) and (7 - 12),

$$(C_{\pi\pi}^{(0)})^2 = 3; \quad (C_{K\bar{K}}^{(0)})^2 = 2; \quad (C_{K\bar{K}}^{(1)})^2 = 2; \quad \left(C_{\pi\eta}^{(1)}\right)^2 = \frac{2}{\sqrt{3}}. \quad (27)$$

We start with the one-threshold situation and choose the channel  $\pi\pi$ , neglecting its connection to  $K\bar{K}$ . In this case one has the following basic elements, with notation  $g_2(\pi\pi, E) \equiv g_\pi$ ,  $\tilde{g}_1(E, \mathbf{P} = 0) = g_1$ , where we keep the lowest pole  $M_1$ , with the notation  $V_{q\bar{q}|\pi\pi} = V_{1\pi} = V_{\pi 1}$

$$k^{(0)}(n\bar{n}|\pi\pi) = (V_{1\pi})^2 = \frac{(C_{\pi\pi}^{(0)})^2 M(\lambda) (f_s^{(1)})^2}{f_\pi^4} = (V_{1\pi})^2, \quad g_1 = \frac{M_1^2}{M_1^2 - E^2}, \quad (28)$$

and the infinite series for the total  $\pi\pi$  Green's function reads, see Fig.3

$$G_{\pi\pi} = g_\pi + g_\pi V_{\pi 1} g_1 V_{1\pi} g_\pi + g_\pi V_{\pi 1} g_1 V_{1\pi} g_\pi V_{\pi 1} g_1 V_{1\pi} g_\pi + \dots, \quad (29)$$

which can be summed up in the form

$$G_{\pi\pi} = g_\pi + g_\pi V_{\pi 1} \frac{1}{1 - g_1 V_{1\pi} g_\pi V_{\pi 1}} g_1 V_{1\pi} g_\pi. \quad (30)$$

For the  $\pi\pi$  scattering amplitude  $f_\pi(e)$ , since  $g_\pi$  does not contain  $\pi\pi$  interaction, one can define

$$G_{\pi\pi} = g_\pi + g_\pi f_\pi(E) g_\pi,$$

and one has

$$f_\pi(E) = \frac{1}{16\pi} V_{\pi 1} \frac{1}{1 - \square_\pi} g_1 V_{1\pi}, \quad (31)$$

where we have defined the 4-term code  $\square_\pi \equiv g_1 V_{1\pi} g_\pi V_{\pi 1} = g_1 g_\pi k^{(0)}(n\bar{n}|\pi\pi)$ .

In an analogous way one can define the one-channel  $K\bar{K}$  Green's function and amplitude

$$f_K(E) = \frac{1}{16\pi} V_{K 1} \frac{1}{1 - \square_K} g_1 V_{1K}, \quad (32)$$

where

$$\square_K = g_1 g_K k^{(0)}(n\bar{n}|K\bar{K}), \quad k^{(0)}(n\bar{n}|K\bar{K}) = \left( \frac{C_{K\bar{K}}^{(0)} M(\lambda) f_s^{(1)}}{f_K} \right)^2. \quad (33)$$

Note, that the  $q\bar{q}$  pole at  $E^2 = M_1^2$  is cancelled in (31), (32); the only visible singularity is the unitary cut in  $g_\pi$  and  $g_K$  respectively.

One can check the unitarity of both amplitudes  $f_\pi$  and  $f_K$ ,

$$\text{Im } f_\pi(E) = \frac{2k_\pi}{E} |f_\pi(E)|^2 \quad (34)$$

and the similar form for  $f_K$  is valid with replacement  $\pi \rightarrow K$ .

One can also find the position of the pole in the amplitude  $f_\pi(E)$  from the denominator in (31),  $\square_\pi(E) = 1$ . One has

$$g_\pi k^{(0)}(n\bar{n}|\pi\pi) \frac{M_1^2}{M_1^2 - E^2} = 1, \quad g_\pi(E) = \text{Re } g_\pi + i \text{Im } g_\pi. \quad (35)$$

We take here  $M_1 = 1.05$  GeV as follows from (21).

In the real part of  $g_\pi(E)$  the cut-off  $N$  is taken at large momenta in (23), equal to the minimal length  $\lambda$ ,  $N = 1/\lambda$ , which yields ( $N = 1$  GeV).

$$g_\pi(E) \approx 0.033 + i0.02 \sqrt{1 - \frac{0.078}{E^2}}. \quad (36)$$

Inserting in (35) for  $I = 0$ ,  $f_\pi = 93$  MeV,  $f_s^{(1)} = 125$  MeV (see Appendix 1 for the discussion of  $f_s^1$  and Appendix 3 for the pole position in the complex plane), and  $M(\lambda = 1 \text{ GeV}^{-1}) = 180$  MeV,  $(C_{\pi\pi}^{(0)})^2 = 3$ , one obtains the equation

$$E^2 = M_1^2 (1 - 20.3 g_\pi(E)), \quad (37)$$

or using (36), one obtains the resonance position  $E_\pi = (0.67 - i0.45)$  GeV ( $\lambda = 1$  GeV $^{-1}$ ). As a result, varying  $\lambda$  in the range  $(1 \div 1.5)$  GeV $^{-1}$  one obtains the resonance parameters

$$E_\pi = (0.6 \div 0.8) \text{ GeV} - i(0.2 \div 0.45) \text{ GeV}. \quad (38)$$

Note, that the resonance appears on the second sheet of the complex plane with respect to the  $\pi\pi$  threshold, as it is explained in Appendix 3.

This can be favorably compared with the experimental values  $f_0(500)$ ,  $E = (400 - 550)$  MeV,  $\Gamma = 400 \div 700$  MeV [1]. Note that we have obtained these values, however, with several simplifying approximations, including the neglect of higher levels in  $g_1$ , possible coupling with the  $K\bar{K}$  channel and notably neglecting the  $4\pi, 6\pi, \dots$  vertices of the chiral theory, which imply the  $\pi\pi$  interaction in  $g_\pi(E)$ . Therefore, the resonance position and the width are subject to essential changes, if one takes this interaction into account. In particular, one can notice, that the resonance position (38) is some  $(150 - 200)$  MeV higher, than in experiment.

We now turn to the  $K\bar{K}$  channel, again neglecting connection to the  $\pi\pi$  channel and keeping only the lowest mass eigenvalue  $M_1 = 1.05$  GeV in  $g_1(E)$ . Inserting in (32)  $(C_{K\bar{K}}^{(0)})^2 = 2$ ,  $f_K = 115$  MeV,  $M(\lambda = 1 \text{ GeV}^{-1}) = 180$  MeV, and  $f_s = 125$  MeV, one obtains  $k^{(0)}(n\bar{n} K\bar{K}) = 5.8$ . From (32) one finds the equation for the pole position,  $\square_K = 1$ , or

$$E^2 = M_1^2(1 - 5.8 g_K(E)), \quad (39)$$

where  $g_K(E)$  with the upper limit  $N = 1$  GeV in (25)

$$g_K(E) = 0.018 + i0.02 \sqrt{\frac{E^2 - 4m_K^2}{E^2}}, \quad (40)$$

which yields an approximate position of the pole

$$E_K = (\lambda = 1 \text{ GeV}^{-1}) = (0.984 - i0.013) \text{ GeV}. \quad (41)$$

One can see that the pole  $E_K$  can be associated with the standard  $f_0(980)$  [1]

$$M(f_0(980)) = (990 \pm 20) \text{ MeV}, \quad \Gamma = (10 \div 100) \text{ MeV}, \quad (42)$$

while the obtained width is inside the allowed region. It is interesting that in this case the cut-off  $\lambda$  in the range  $(0.5 \div 2)$  GeV $^{-1}$  brings about only few percent change in the resulting resonance parameters. Taking into account the approximations made above, this agreement can be considered as reasonable,

however, one should take into account, that both channels  $\pi\pi$  and  $K\bar{K}$  should be connected, as it is seen in the experimental measurements of the ratio for  $f_0(980)$ ,  $\frac{\Gamma(K\bar{K})}{\Gamma(\pi\pi)} = 0.69 \pm 0.32$  [1].

The standard way to include the  $\varphi\varphi$  channel coupling is to write for the amplitudes  $\hat{f}_{\alpha\beta} = \begin{pmatrix} f_{\pi\pi} & f_{\pi K} \\ f_{K\pi} & f_{KK} \end{pmatrix}$  the  $K$  matrix form,

$$\hat{f}^{-1} = 16\pi \begin{pmatrix} \frac{1-\square_\pi}{w_\pi} & a \\ b & \frac{1-\square_K}{w_K} \end{pmatrix}, \quad w_\pi = V_{\pi 1} g_1 V_{1\pi}, \quad w_K = V_{k_1 g_1} V_{iK}. \quad (43)$$

As a result one obtains

$$\hat{f} = \frac{1}{16\pi} \frac{\begin{pmatrix} \frac{1-\square_K}{w_\pi} & -b \\ -a & \frac{1-\square_\pi}{w_K} \end{pmatrix}}{\frac{1-\square_\pi}{w_\pi} \cdot \frac{1-\square_K}{w_K} - ab}, \quad (44)$$

and in the limit  $ab = 0$  one returns to the two independent channels.

One can check that the amplitudes  $f_{\alpha\beta}$ ,  $\alpha, \beta = \pi\pi, K\bar{K}$  satisfy the unitarity relations with the normalization factor  $\text{Im } g_{\pi,K} = \frac{k_{\pi,K}(E)}{8\pi E}$ . In particular for the  $f_{K\bar{K}}$  one has in this channel coupling (CC) form

$$16\pi f_{K\bar{K}} = \frac{(1 - \square_\pi)w_K}{(1 - \square_\pi)(1 - \square_K) - abw_K w_\pi} \quad (45)$$

Estimating the  $w_K, w_\pi$  one finds that the CC can affect the positions and the widths of the uncoupled resonances (38), (41) and therefore this point should be studied in more detail.

We shall start with the  $f_{\pi\pi}$  amplitude, which can be written as follows

$$16\pi f_{\pi\pi} = \frac{\frac{1}{w_K} - g_K}{\left(\frac{1}{w_\pi} - g_\pi\right) \left(\frac{1}{w_K} - g_K\right) - ab}, \quad (46)$$

and we can rewrite (46) as follows using  $\gamma = 40.4 ab$  and the properly normalized amplitudes  $\text{Im } f_\pi^{(0)} = \frac{2k}{E} |f_\pi^{(0)}|^2$

$$f_\pi^{(0)} = \frac{1}{\frac{16\pi}{k} \frac{(E_\pi^2 - E^2)}{M_1^2} - \frac{\gamma M_1^2}{E_K^2 - E^2}} \quad (47)$$

with

$$E_\pi^2 = M_1^2 \left(1 - k^{(0)}(n\bar{n}|\pi\pi)g_\pi\right), \quad E_K^2 = M_1^2 \left(1 - k^{(0)}(n\bar{n}|K\bar{K})g_K\right). \quad (48)$$

Analogously for  $f_K^{(0)}$  one has

$$f_K^{(0)} = \frac{1}{\frac{16\pi}{kM_1^2}(E_K^2 - E^2) - \frac{2.34\gamma M_1^2}{E_\pi^2 - E^2}}. \quad (49)$$

One can estimate the ratio of imaginary parts of the first and the second term in the denominator of (49), which yields the order of magnitude of the ratio of  $\Gamma_{K\bar{K}}(f(980))$  and  $\Gamma_{\pi\pi}(f(980))$  at  $E = 1.00$  GeV,

$$\frac{\Gamma_{\pi\pi}(f(980))}{\Gamma_{K\bar{K}}(f(980))} \cong \frac{2.4\gamma\sqrt{E^2 - 4m_\pi^2}}{\sqrt{E^2 - 4m_K^2}} \approx 17\gamma \quad (50)$$

and one can see that this ratio is around 1 for  $\gamma = 0.05$ , found in the next section by comparison with data. The resulting pole is near the  $K\bar{K}$  threshold and satisfies the criteria of the  $f^{(0)}(980)$  resonance.

## 5 Results and discussion

From (47) one can see that the amplitude  $f_\pi^{(0)}$  can be expressed via the Green's functions  $g_\pi$  and  $g_K$  with the only parameter  $\gamma$ , responsible for the coupling of channels  $\pi\pi$  and  $K\bar{K}$ . Note, that the only parameter  $\lambda$  enters both  $q\bar{q} - m\bar{m}$  coupling  $k^{(0)}$  and the real parts of both Green's functions, which start and finish at the same distance  $\lambda$  and therefore contain the legitimate factor  $N \sim 1/\lambda \sim O(1 \text{ GeV})$ . In the present paper we have chosen  $\lambda$  in the narrow interval around  $1 \text{ GeV}^{-1}$ , which has yielded reasonable results. In the subsequent paper [56] it was shown, that  $\lambda$  can be defined from the stationary point of the transition coefficient  $k^{(0)}$  and indeed has value near  $0.2 \text{ Fm} = 1 \text{ GeV}^{-1}$ .

The main result of our approach, based on the CCL (1), is that the  $q\bar{q}$  pole at 1 GeV can provide only one resonance, when connected with one threshold, and we need  $\pi\pi - K\bar{K}$  channel coupling to produce two quark-chiral resonances:  $f_0(500)$  due to coupling  $n\bar{n} - \pi\pi$ , and  $f_0(980)$  due to coupling  $n\bar{n} - K\bar{K}$  ( $n = u, d$ ). This is a feature of our quark-chiral Lagrangian, and is obtained from the infinite sums of products of  $\square_\pi$  and  $\square_K$ . Starting with uncoupled  $\pi$  and  $K$  channels, it is interesting that the  $\pi\pi$  pole, produced by the  $q\bar{q}$  pole obtains without the  $\pi\pi$  interaction, which is governed by the chiral Lagrangian, however, far from experimental position, and then one needs direct (not via  $q\bar{q}$ )  $\pi\pi$  interaction to bring resonance to the realistic values, which can be obtained directly by the analysis in [30, 31, 32]. The possible reason is that the low energy physics is only mildly connected to the higher  $f^{(0)}$  resonance physics, but strongly affects



low and intermediate energy region, including  $f_0(500)$  position, and we have neglected at the first stage the low energy  $\pi\pi$  interaction given by the chiral Lagrangian.

Therefore, in our general two-channel form we include a possible modification of real and imaginary part of  $g_\pi$  due to direct  $\pi\pi$  or  $K\bar{K}$  interaction, which is contained in the term  $E_\pi^2$  in (48), which leads to the following two-channel form, generalizing (47),

$$f_\pi = \frac{1}{2.67 \frac{\tilde{E}_\pi^2 - E^2}{M_1^2}} - \frac{\gamma M_1^2}{E_K^2 - E^2}; \quad \tilde{E}_\pi^2 = M_1^2 \left( 1 - x(E) - iy(E) \sqrt{\frac{E^2 - 4m_\pi^2}{E^2}} \right) \quad (51)$$

$$F_2(E) = 0.96 - 0.043 i \sqrt{1 - \frac{0.975}{E^2}} \theta(E^2 - 0.975) - E^2 \quad (52)$$

Here  $x(E) = k \operatorname{Re} g_\pi(E)$ ,  $y = k \operatorname{Im} g_\pi(E)$  are found by fitting the resulting curves of  $\operatorname{Re} f_\pi^{(0)}$ ,  $\operatorname{Im} f_\pi^{(0)}$  to the data of [31, 32]. Parameters of  $x(E)$ ,  $y(E)$  are given in the Appendix A3.

The two curves  $f_\pi(E)$ , obtained by the fitting of  $g_\pi(E)$ , are shown in Figs. 4 and 5 by the solid lines together with the curves from the paper of Pelaez et al. [31], obtained in the course of the analysis in [32]. In the same figures we show the dashed line curves obtained from (47),(48) with the free  $\pi\pi$  Green's function. As one can see, our  $\operatorname{Re} f_\pi^{(0)}(E)$  and  $\operatorname{Im} f_\pi^{(0)}(E)$  for the free case are in a qualitative agreement with the results of [31], with an exclusion of the region of relatively small energies,  $E < 0.5$  GeV.

This means that the  $\pi\pi$  interaction is important in this region and the approximation of the free  $\pi\pi$  Green's function should be modified by inclusion of the purely chiral interactions at least for the lowest  $f_0(500)$  resonance.

This is well illustrated by the calculation of the position of the resonance  $f_0(500)$ , which was obtained above in the free  $g_\pi$  case at  $(0.67 - i0.45)$  GeV, while from [31] ( the dotted lines in Figs 5,6) the resonance position is at  $(0.457 - i0.259)$  GeV.

However, it was not the purpose of our study to reproduce exactly the  $\pi\pi$  interaction amplitude in the whole region (280, 1000) MeV, but rather to discover the dynamical mechanism, producing the lowest scalar-isoscalar mesons  $f_0(500)$  and  $f_0(980)$ . As shown, at the first stage this mechanism can be reduced in its basic part to the interaction of the  $q\bar{q}$  and free meson-meson channels, given by our quark-chiral interaction in the CCL, Eq. (1). Indeed, this

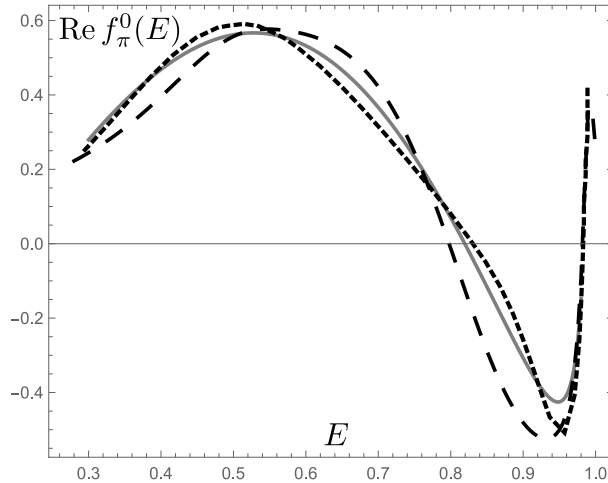


Figure 5:  $\text{Re } f_{\pi}^{(0)}(E)$  as a function of  $E$  in GeV from Eq. (47) (grey bands) in comparison with the resulting curves from the Pelaez et al. [31, 32] (broken lines) comprising the  $\pi\pi$  data.

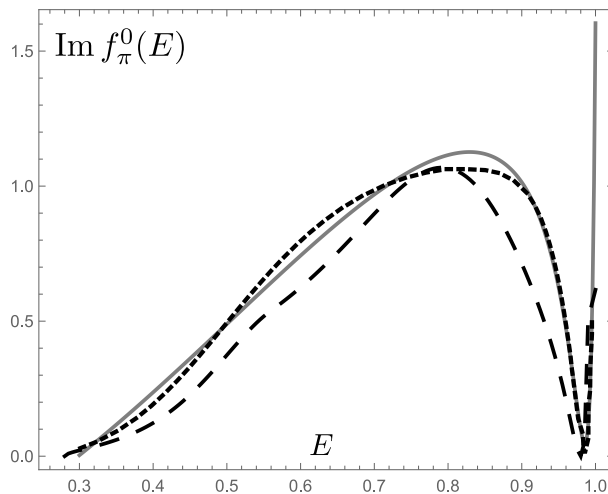


Figure 6: The same as in Fig. 4, but for  $\text{Im } f_{\pi}^{(0)}(E)$ .

interaction provides the reasonable coupling  $V_{q\bar{q}|\pi\pi}$  and  $V_{q\bar{q}|K\bar{K}}$ , in addition to the values of the  $q\bar{q}$  Green's functions and the corresponding poles  $M_n(q\bar{q})$ . In our case the lowest pole  $M_1(q\bar{q})$  at 1 GeV produces a wide resonance  $f_0(500)$  in “collaboration” with the  $\pi\pi$  Green's function and the  $\pi\pi$  threshold, and a more narrow resonance  $f_0(980)$  in “collaboration” with the  $K\bar{K}$  Green's function and the threshold. The interaction of these two channels, strongly shifted in energy from each other, which is outside our simple  $q\bar{q}$ -meson-meson model, only slightly modifies their individual properties, as can be seen comparing one-channel and coupled-channel characteristics.

As the second stage one should take into account the chiral interactions ( $\pi\pi, K\bar{K}$ ) to obtain the relativistic  $\pi\pi$  and  $K\bar{K}$  amplitudes. This stage is especially essential for the determination of the  $f_0(500)$  pole parameters, as can be seen from the analysis in [31],  $E = (457 \pm 10) \text{ MeV} - i279 \text{ MeV}$ , which agrees with the results of [30]. This result disagrees with our estimate (38), where the  $\pi\pi$  interaction was disregarded. At the same time the characteristics of the  $f_0(980)$  in [31] and in our case, Eq. (41) are similar. This leads to the conclusion, that the accurate determination of lowest resonances, much below 1 GeV, requires the proper account of the  $\varphi\varphi$  interaction, which can be done combining the formalism of [30, 31], with our  $q\bar{q} - \varphi\varphi$  approach.

This is the main concrete result of this paper, however, the general mechanism, described above, leads to many further possible discoveries.

At this point one can immediately ask: if the same  $q\bar{q}$  level can create several resonances, accounting for the coupling between  $\varphi\varphi$  channels, what happens with  $a_0(980)$  resonance, which can decay both to  $\pi\eta$  and  $K\bar{K}$ , but in experiment one can see only one broad resonance near the  $K\bar{K}$  threshold. Now we apply our technique to this case to understand the difference between the situation with  $a_0(980)$  on one hand and  $f_0(500), f_0(980)$  on another.

To this end we shall try to find separate resonances in the  $\pi\eta$  and  $K\bar{K}$  channels and write, as in (37), the resulting equation for the position of the assumed resonances  $E^{(1)}(\pi\eta)$  and  $E^{(1)}(K\bar{K})$ , where the upper index refers to the isospin  $I = 1$ .

$$(E^{(1)}(\nu))^2 = M_1^2(1 - k^{(1)}(n\bar{n}|\nu)g_\nu(E)); \quad \nu = \pi\eta, K\bar{K}. \quad (53)$$

Now using (28) and (8)-(12) one can write:

$$k^{(1)}(n\bar{n}|\pi\eta) \approx V_{\pi\eta,1}V_{1,\pi\eta} = (C_{\pi\eta}^{(1)})^2 \frac{M^2(\lambda)(f_s^{(1)})^2}{f_\pi^2 f_\eta^2} = 4.69 \quad (54)$$

$$k^{(1)}(n\bar{n}|K\bar{K}) = \frac{(C_{K\bar{K}}^{(1)})^2 M^2(\lambda) (f_s^{(1)})^2}{f_K^4} = 2.9 \quad (55)$$

(We have neglected the difference between  $f_\pi$  and  $f_\eta$  for a rough estimate, in the real case the coefficient in (54) is smaller).

Now  $g_{\pi\eta}(E)$  has a smaller real and imaginary parts, (see Appendix 2 for details) as compared with  $g_{\pi\pi}(E)$  Eq. (36), while  $g_{K\bar{K}}(E)$  is the same as was used before, see Eq.(40). As a result, the solution of Eq. (53) gives two resonances

$$E^{(1)}(\nu) = M_1(1 - \bar{a}_\nu - i\bar{b}_\nu), \quad (56)$$

where a rough estimate yields

$$\bar{a}_{\pi\eta} \cong 0.05, \quad \bar{b}_{\pi\eta} \approx 0.05 \quad (57)$$

$$\bar{a}_{K\bar{K}} = 0.022, \quad \bar{b}_{K\bar{K}} = 0.04\sqrt{\frac{E^2 - 4m_K^2}{E^2}}. \quad (58)$$

One should take into account that  $M_1(I = 1) \approx M_1(I = 0) = 1.00$  GeV and obtains  $E^{(1)}(\pi\eta) \cong (1.05)$  GeV, while  $E^{(1)}(K\bar{K}) \cong \left(1.04 - i0.02\sqrt{\frac{E^2 - 4m_K^2}{E^2}}\right)$  GeV, and  $E^{(1)}(\pi\eta)$  is on the second sheet with the  $\pi\eta$  threshold, while  $E^{(1)}(K\bar{K})$  on the second sheet with the  $K\bar{K}$  threshold.

One should however take into account the  $\pi\eta - K\bar{K}$  channel coupling, which can rearrange the position of the poles, as it was found recently in the lattice calculations [14].

Thus, one can see that the displacements of both resonances are small, being of the order of the width of resonances. This might be the reason why in experiment one actually observes one resonance  $a_0(980)$  near 1 GeV with two decay modes, while in the  $I = 0$  channel with larger couplings  $k^{(0)}(n\bar{n}|\pi\pi)$  and more distant  $\pi\pi$  and  $K\bar{K}$  thresholds one observes two distinct resonances, and this example gives an additional support for our theory.

## 6 Conclusions and an outlook

First of all, comparing our approach with other models, one should stress that we neglect any direct  $\varphi\varphi$  interaction in the first step, described in the paper. Therefore, all details of this interaction, as well as  $q\bar{q} - q\bar{q}$  interaction, in particular crossing symmetry, the left-cut singularities etc are missing in this first step. As a second, and a more complicated step, one should take into account all

details of the  $\varphi\varphi$  interaction, e.g. as in the dispersive methods or in unitarized chiral model interaction.

Summarizing, the method suggested above as a first stage, has a general character and can be applied to any systems, consisting of several components, which can transform one into another. The only information, needed to describe the properties of such mixed systems, is the spectral properties of each component and transition coefficients. In the case of the charmonium system this method has given a first explanation of the resonance  $X(3872)$  [42]. In the case of the quark-chiral system,  $q\bar{q} - \varphi\varphi$ , this method uses the information given by the FCM approach plus quark-chiral CCL Lagrangian (1). As it is, our method suggests a possible solution of the old-standing problem of  $f_0(500)$ ,  $f_0(980)$  and  $a_0(980)$  associating these resonances with ( $n = 1$ )  $q\bar{q}$   $^3P_0$  states.

As applied to the lowest scalar resonances, we have shown that the resonances  $f_0(500)$  and  $f_0(980)$ , as well as the  $a_0(980)$  resonance, can be connected with the use of CCL, to the  $n = 1$ ,  $M \approx 1$  GeV  $q\bar{q}$  resonance calculating explicitly the transition coefficients and consequently the partial widths. Then several questions arise:

1. Since we have connected  $f_0(500)$ ,  $f_0(980)$  with one  $q\bar{q}$  state – the  $^3P_0$  ground state  $n\bar{n}$  with mass around 1 GeV, one should consider the next  $q\bar{q}$  state,  $M_2(1474)$  as an excited  $q\bar{q}$  state with  $n = 2$ , in contrast to an accepted view (see [1]) that this latter is a ground state. It is interesting to study consequences of this assignment.
2. What will be the result for excited  $q\bar{q} - \varphi\varphi$  states, e.g. with  $M_2 = 1474$  MeV, in connection with the same  $\varphi\varphi$  thresholds and can one expect more additional resonances below  $M_2$  ?
3. It is clear that taking into account the full sum  $\sum_n \frac{M_n^2}{M_n^2 - E^2}$  one meets with divergences and with the necessity of renormalization. This probably can be treated in the spirit of the formalism, developed in the method of Matrix Product States (MPS), see [54] for reviews.
4. We have considered above only one  $q\bar{q}$  channel. However, for the  $K\bar{K}$  system the  $s\bar{s}$  channel provides bound states starting with  $M_1 \cong 1400$  MeV, just near the first excited  $n\bar{n}$  state. Therefore, for the  $K\bar{K}$  system one should take into account both  $n\bar{n}$  and  $s\bar{s}$  states, which requires an extension of our method with inclusion of several  $q\bar{q}$  and one or more  $\varphi\varphi$  channels to explain several extra resonances in the region 1300-1700 MeV, observed in experiment [1].

These topics have been recently studied in [56] as our subsequent paper and it was shown, how excited  $q\bar{q}$  states produce higher scalar resonances using the explicit method, discussed in the present paper. In addition, also  $n\bar{s}$  and  $s\bar{s}$  systems have been considered in connection with the corresponding  $mm$  thresholds and the same picture of the pole shifts as in the present paper was found. From this point of view our approach helps to clarify the old problem of scalar resonances both in the ground and first excited states, leaving the question: what parts in lowest scalars are occupied by  $q\bar{q}$  and direct  $\varphi\varphi$  interactions for a future investigation.

This work was done in the frame of the scientific project, supported by the Russian Science Foundation grant number 16-12-10414. The authors are indebted to A.M. Badalian for many discussions, suggestions and details, which are used in the paper. Discussions with Yu.S. Kalashnikova and Z.V. Khaidukov are gratefully acknowledged.

## Appendix A1. Decay constants of scalar mesons

In the framework of the path-integral formalism the decay constants of the  $q\bar{q}$  meson states can be defined as in [39, 49]

$$(f_{\Gamma}^{(n)})^2 = \frac{2N_c \langle Y_{\Gamma} \rangle |\varphi_n(0)|^2}{\omega_1 \omega_2 M_n}, \quad (\text{A1.1})$$

where  $\omega_1, \omega_2$  are average energies of quarks with masses  $m_1$  and  $m_2$ ,  $M_n$  is the mass of the meson,  $\varphi_n(r)$  is the (relativistic) meson wave function of the relative distance  $r$ , while  $\langle Y_{\Gamma} \rangle$  is

$$4Y_{\Gamma} = \text{tr}((m_1 - \hat{D}_1)\Gamma(m_2 - \hat{D}_2)\Gamma) = \text{tr}((m_1 - i\hat{p}_1)\Gamma(m_2 + i\hat{p}_2)\Gamma). \quad (\text{A1.2})$$

Here  $\Gamma$  is the vertex operator, for the scalar particle  $\Gamma_s = 1$ , but the momentum operators  $\hat{p}_i$  are acting on the wave function  $\varphi_n(r)$ , namely  $ip_i\varphi_n(r) = \partial_i\varphi_n(r)$ . In our case

$$\langle Y_s \rangle |\varphi_n(0)|^2 = (m_1 m_2 - \omega_1 \omega_2 - \hat{\mathbf{p}}\hat{\mathbf{p}}') |\Psi_S(0)|^2 \rightarrow (\partial_i \Psi_S(\mathbf{r}) \partial'_i \Psi_S^*(\mathbf{r}'))_{r \rightarrow 0, r' \rightarrow 0}. \quad (\text{A1.3})$$

Since  $\Psi_S(\mathbf{r})$  is

$$\Psi_S(\mathbf{r}) = \sum \chi_{1M_1} \tilde{Y}_{1m_2} \frac{\varphi(r)}{r} C_{1m_1, 1m_2}^{00} \quad (\text{A1.4})$$

and  $\tilde{Y}_{1m} \equiv rY_{1m}$ , after summation over spin projections one finds

$$\partial_i \Psi_S(\mathbf{r}) \partial'_i \Psi_S^*(\mathbf{r}') = \partial_i \partial'_i \frac{1}{4\pi} (xx' + yy' + zz') = \frac{1}{4\pi} \quad (\text{A1.5})$$

where we have taken into account, that the subscript  $i$  refers to a fixed momentum direction. As a result one obtains

$$(f_S^{(n)})^2 = \frac{2N_c (R'_{nP}(0))^2}{4\pi\omega_1\omega_2 M_n}, \quad (\text{A1.6})$$

where  $R'_{nP}(0) = \left( \frac{\varphi_n(r)}{r} \right)_{r \rightarrow 0}$ . Estimated in the same way as in [39, 49] for the  $1P$  scalar state one has  $R'_{1P}(0) = 0.086 \text{ GeV}^{5/2}$ ,  $\omega_1 = \omega_2 = 0.448 \text{ GeV}$  [55] and according to (A1.6) one obtains

$$(f_S^{(1)})^2 = 0.01568 \text{ GeV}^2, \quad f_S^{(1)} = 0.125 \text{ GeV}. \quad (\text{A1.7})$$

For the first excited state,  $2P$ , one has for the scalar state  $\omega(2P) \cong 0.5 \text{ GeV}$ ,  $R'_{2P}(0) = 0.0817 \text{ GeV}^{5/2}$ ,  $M(2P) = 1.474 \text{ GeV}$  [55].

As a result one obtains from (A1.6)

$$(f_s^{(2)})^2 = 0.00865 \text{ GeV}^2, \quad f_s^{(2)} = 0.093 \text{ GeV}. \quad (\text{A1.8})$$

## Appendix A2. Meson-meson Green's functions

The relativistic Green's function of two scalar mesons with the total momentum  $P$  can be written in the Euclidean space-time as

$$g(P) = \int \frac{d^4 p}{(2\pi)^4} \frac{1}{[(P-p)^2 + m_1^2](p^2 + m_2^2)}. \quad (\text{A2.1})$$

Integrating over  $dp_4$  in the c.m. frame,  $\mathbf{P} = 0$ , one obtains, with  $P_4 = iE$ , and  $m_1 > m_2$ ,

$$\begin{aligned} \text{Re } g_{12}(E) &= \int_0^N \frac{p^2 dp}{4\pi^2} \times \\ &\times \frac{E(\sqrt{p^2 + m_1^2} + \sqrt{p^2 + m_2^2}) + m_1^2 - m_2^2}{\sqrt{p^2 + m_1^2} \sqrt{p^2 + m_2^2} [(\sqrt{p^2 + m_1^2} + \sqrt{p^2 + m_2^2})^2 - E^2] (E + \sqrt{p^2 + m_1^2} - \sqrt{p^2 + m_2^2})} \end{aligned} \quad (\text{A2.2})$$

Here we have introduced the cut-off  $N$  in momentum  $p$ .

$$\text{Im } g(E) = \frac{1}{16\pi} \frac{\sqrt{(E^2 - (m_1 + m_2)^2)(E^2 - (m_1 - m_2)^2)}}{E}. \quad (\text{A2.3})$$

In the equal mass limit one obtains

$$\text{Re } g(E) = \int_0^N \frac{p^2 dp}{8\pi^2 \sqrt{p^2 + m^2} (p^2 + m^2 - E^2/4)}, \quad (\text{A2.4})$$

which for  $E^2 = 4m^2$  reduces to a simple answer

$$\text{Re } g(2m) = \frac{1}{8\pi^2} \int_0^N \frac{dp}{\sqrt{p^2 + m^2}} = \frac{1}{8\pi^2} \ln \frac{N + \sqrt{N^2 + m^2}}{m}. \quad (\text{A2.5})$$

For  $E^2 = 4m^2 - 4\Delta$ ,  $\Delta > 0$  one has instead of (A2.5)

$$\text{Re } g(E) = \frac{1}{8\pi^2} \int_0^N \frac{dp}{\sqrt{p^2 + m^2}} - \frac{\Delta}{8\pi^2} \int_0^N \frac{dp}{\sqrt{p^2 + m^2} (p^2 + \Delta)}. \quad (\text{A2.6})$$

and for  $m^2 \gg \Delta$  the last integral in (A2.6) can be written as

$$\Delta \text{Re } g(E) \cong -\frac{\sqrt{\Delta}}{16\pi m} \theta \left( m^2 - \frac{E^2}{4} \right). \quad (\text{A2.7})$$

Note, that  $\Delta \text{Re } g(E)$  is much smaller than  $\text{Re } g(2m)$ , Eq. (A2.5) and can be neglected in the first approximation.

## Appendix A3. Position of new poles in the complex plane

One can write the equation (37) for the  $\pi\pi$  pole as

$$E^2 = M_1^2 (1 - \text{const}(\text{Re } g_\pi(E)) + i \text{const}(\text{Im } g_\pi(E))) \quad (\text{A3.1})$$

Writing  $\text{Im } g_\pi(E) = \text{const } p(E)/E$ , where  $p(E) = \sqrt{E^2 - 4m_\pi^2}$ , one can rewrite (A3.1) as  $E^2 = E_0^2 - \frac{ibp(E)}{E}$ , or else expressing  $E^2$  via  $p^2$  one has

$$p^2(E) + \frac{ibp(E)}{\sqrt{p^2(E) + 4m_\pi^2} - p_0^2} = 0 \quad (\text{A3.2})$$



where  $b$  and  $p_0$  are constants. Starting with small  $b$  one will have approximately  $p(E) = p_0$ , and in the next order having  $\sqrt{p^2(E) + 4m_\pi^2} = \sqrt{P_0^2 + 4m_\pi^2}$ , one solves the quadratic equation for  $p(E)$  as

$$p(E) = -\frac{ib}{2\sqrt{p^2(E) + 4m_\pi^2}} \pm \sqrt{\frac{-b^2}{4(\sqrt{p^2(E) + 4m_\pi^2})^2} + p_0^2} \quad (\text{A3.3})$$

One can do next orders of approximations following the motion of the root, starting with the position (A3.3). Another way is the direct solution of the equation (A3.2) which is cubic in  $p^2(E)$  choosing the correct root to be consistent with (A3.3). As it is seen in (A3.3) the sign of imaginary part of  $p(E)$  is negative, implying that the pole is on the second sheet in the  $E$ -plane, corresponding to the  $\pi\pi$  threshold.

## References

- [1] M. Tanabashi, K. Hagiwara, K. Hikasa, et al., (Particle Data Group) Phys. Rev. **D 98**, 030001 (2018).
- [2] F. E. Close and N. A. Tornqvist, J. Phys. **G 28**, 249 (2002) [hep-ph/0204205].
- [3] D. V. Bugg, Phys. Rept. **397**, 257 (2004).
- [4] C. Amsler and N. A. Tornqvist, Phys. Rept. **389**, 61 (2004).
- [5] R. L. Jaffe, Phys. Rept. **409**, 1 (2005).
- [6] E. Klempt and A. Zaitsev, Phys. Rept. **454**, 1 (2007) [arXiv:0708.4016].
- [7] N. N. Achasov, Phys. Usp., **41**, 1149 (1998) [hep-ph/9904223];  
N. N. Achasov, Nucl. Phys. **A 675**, 279 (2000) [hep-ph/9910540].
- [8] J. R. Peláez, Phys. Rept. **658**, 1 (2016) [arXiv:1510.00653].
- [9] N. N. Achasov and G. N. Shestakov, Phys. Usp., **62**, 3 (2019) [arXiv:1905.11729].
- [10] R. L. Jaffe, Phys. Rev. **D 15**, 267 (1977);  
R. L. Jaffe, Phys. Rev. **D 15**, 281 (1977);  
G.'t Hooft, G. Isidori, L. Maiani, et al., Phys. Lett. **B 662**, 424 (2008)

- [arXiv:0801.2288];  
D. Ebert, R. N. Faustov, and V. O. Galkin, Eur. Phys. J. **C 60**, 273 (2009)  
[arXiv:0812.2116];  
G. Eichmann, C. Fischer, and W. Heupel, Phys. Lett. **B 753**, 282 (2016)  
[arXiv:1508.07178].
- [11] J. D. Weinstein and N. Isgur, Phys. Rev. Lett., **48**, 659 (1982);  
J. D. Weinstein and N. Isgur, Phys. Rev. **D 27**, 588 (1973);  
J. D. Weinstein and N. Isgur, Phys. Rev. **D 41**, 2236 (1990);  
Yu. S. Kalashnikova and A. V. Nefediev, Phys. Usp. **62**, 568 (2019)  
[arXiv:1811.01324].
- [12] Z. G. Wang, Eur. Phys. J. **C 76**, 427 (2016) [arXiv: 1507.02131].
- [13] M. G. Alford and R. L. Jaffe, Nucl. Phys. B **B 578**, 367 (2000),  
[hep-lat/0001023];  
H. Suganuma, K. Tsumura, N. Ishii and F. Okiharu, Prog. Theor. Phys.  
Suppl. **168**, 168 (2007) [arXiv:0707.3309];  
N. Mathur, A. Alexandru, Y. Chen, et al., Phys. Rev. **D 76**, 114505 (2007)  
[hep-ph/0607110];  
M. Loan, Z. H. Luo and Y. Y. Lam, – arXiv: 0907.3609;  
S. Prelovsek and D. Mohler, Phys. Rev. **D 79**, 014503 (2009)  
[arXiv:0810.1759];  
T. Kunihiro, S. Muroya, A. Nakamura, et al., [SCALAR Collaboration],  
Phys. Rev. **D 70**, 034504 (2004) [hep-ph/0310312].
- [14] J. J. Dudek, R. G. Edwards, and D. J. Wilson (Hadron Spectrum Collab-  
oration), Phys. Rev. **D 93**, 094506 (2016) [arXiv:1602.05122].
- [15] E. van Beveren, T. A. Rijken, K. Metzger, et al. Z. Phys. **C 30**, 615 (1986)  
[arXiv:0710.4067].
- [16] E. van Beveren and G. Rupp, Eur. Phys. J. **C 22**, 493 (2001)  
[hep-ex/0106077].
- [17] E. van Beveren, D. V. Bugg, F. Kleefeld and G. Rupp, Phys. Lett. **B 641**,  
265 (2006) [hep-ph/0606022].
- [18] N. A. Tornqvist and M. Roos, Phys. Rev. Lett. **76**, 1575 (1996)  
[hep-ph/9511210].

- [19] N. A. Tornqvist, Z. Phys. **C 68**, 647 (1995) [hep-ph/9504372];  
N. A. Tornqvist and M. Roos, Phys. Rev. Lett. **76**, 1575 (1996) [hep-ph/9511210].
- [20] M. Boggione and M. R. Pennington, Phys. Rev. **D 65**, 114010 (2002) [hep-ph/0203149].
- [21] T. Wolkanowski, F. Giacosa, and D. H. Rischke, Phys. Rev. **D 93**, 014002 (2016) [arXiv:1508.00372].
- [22] I. K. Hammer, C. Hanhart and A. V. Nefediev, Eur. Phys. J. **A 52**, 330 (2016) [arXiv:1607.06971].
- [23] J. Oller and E. Oset, Phys. Rev. **D 60** (1999), 074023 doi:10.1103/PhysRevD.60.074023 [hep-ph/9809337].
- [24] J. R. Pelaez and G. Rios, Phys. Rev. Lett. **97**, 242002 (2006) [hep-ph/0610397].
- [25] J. Ruiz De Elvira, J.R. Pelaez, M. R. Pennington and D. J. Wilson, Phys. Rev. **D 84**, 096006 (2011) [arXiv:1009.6204].
- [26] J. Oller and E. Oset, Nucl. Phys. **A 620**, 438 (1997) [hep-ph/9702314].
- [27] A. Dobado and J. Pelaez, Phys. Rev. **D 56**, 3057 (1997) [hep-ph/9604416].
- [28] A. Gomez Nicola and J. Pelaez, Phys. Rev. **D 65**, 054009 (2002) [hep-ph/0109056].
- [29] J. Pelaez, Phys. Rept. **658** (2016) [arXiv:1510.00653].
- [30] J. R. Peláez, F. J. Yndurain, Phys. Rev. **D 71**, 074016 (2005) [hep-ph/0411334];  
R. Garcia-Martin, R. Kaminski, J. R. Peláez et al. Phys. Rev. Lett. **107**, 072001 (2011) [arXiv:1107.1635].
- [31] J. R. Peláez, A. Rodas and J. Ruiz De Elvira, Eur. Phys. J. **C79**, 1008 (2019) [arXiv:1907.13162].
- [32] R. Garcia-Martin, R. Kaminski, J. R. Peláez, J. Ruiz De Elvira, and F.J.Yndurain, Phys. Rev. **D 83**, 074004 (2011) [arXiv:1102.2183].
- [33] A. M. Badalian, Phys. Atom. Nucl. **66**, 1342 (2003) [hep-ph/0302089].

- [34] D. Darvish, R. Brett, J. Bulava, et al., – arXiv:1909.07747.
- [35] A. Di Giacomo, H. G. Dosch, V. I. Shevchenko, and Yu. A. Simonov, Phys. Rept. **372**, 319 (2002) [hep-ph/0007223];  
Yu. A. Simonov, in: “QCD: Perturbative or Nonperturbative?”, Ed. by L. S. Ferreira et al., World Scien. Ed., Singapore, 2001, p. 60 [hep-ph/9911237].
- [36] Yu. A. Simonov, Phys. Rev. **D 99** 056012 (2019) [arXiv:1804.08946].
- [37] Yu. A. Simonov, Phys. Rev. **D 99**, 096025 (2019) [arXiv:1902.05364].
- [38] A. M. Badalian and B. L. G. Bakker, Phys. Rev. **D 100** 034010 (2019) [arXiv:1901.10280].
- [39] A. M. Badalian and B. L. G. Bakker, Phys. Rev. **D 67**, 071901 (2003) [hep-ph/0302200];  
A. M. Badalian, B. L. G. Bakker, and Yu.A.Simonov, Phys. Rev. **D 75**, 116001 (2007) [hep-ph/0702157];  
Yu. A. Simonov, Phys. Rev. **D 88**, 025028 (2013) [arXiv:1303.4952].
- [40] E. Eichten, K. Gottfried, K. Kinoshita, et al., Phys.Rev. **D 17**, 3090 (1978);  
E. Eichten, K. Gottfried, K. Kinoshita, et al., Phys.Rev. **D 21**, 203 (1980).
- [41] E. Eichten, K. Lane and C. Quigg, Phys.Rev. **D 69**, 094019 (2004) [hep-ph/0401210];  
Yu. S. Kalashnikova, Phys. Rev. **D 72**, 034010 (2005) [hep-ph/0506270].
- [42] I. V. Danilkin and Yu. A. Simonov, Phys. Rev. **D 81**, 074027 (2010) [arXiv:0907.1088];  
I. V. Danilkin and Yu. A. Simonov, Phys. Rev. Lett. **105**, 102002 (2010) [arXiv:1006.0211];  
I. V. Danilkin, V. D. Orlovsky and Yu. A. Simonov, Phys. Rev. **D 85**, 0340 (2012) [arXiv:1106.1552].
- [43] Yu. A. Simonov, Phys. Rev. **D 65**, 094018 (2002) [hep-ph/0201170];  
Yu. A. Simonov, Phys. Atom. Nucl. **67**, 846 (2004) [hep-ph/0302090];  
Yu. A. Simonov, Phys. Atom. Nucl. **67**, 1027 (2004) [hep-ph/0305281];  
S. M. Fedorov and Yu. A. Simonov, JETP Lett. **78**, 57 (2003) [hep-ph/0306216].
- [44] Yu. A. Simonov, Int. J. Mod. Phys. **A 31**, 1650104 (2016) [arXiv:1509.06930].

- [45] J. Gasser and H. Leutwyler, *Ann. Phys. (NY)* **158**, 142 (1984);  
 J. Gasser and H. Leutwyler, *Nucl. Phys.* **B 250**, 465 (1985);  
 J. Gasser and H. Leutwyler, *Nucl. Phys.* **B 307**, 763 (1988).
- [46] Yu. A. Simonov, *Phys. Atom. Nucl.* **79**, 265 (2016) [arXiv:1502.07569].
- [47] Yu. A. Simonov, *Phys. Rev.* **D 88**, 025028 (2013) [arXiv:1303.4952].
- [48] Yu. A. Simonov and J. A. Tjon, *Ann. Phys.* **228**, 1 (1993);  
 Yu. A. Simonov and J. A. Tjon, *Ann. Phys.* **300**, 54 (2002)  
 [hep-ph/0205165].
- [49] A. Yu. Dubin, A. B. Kaidalov and Yu. A. Simonov, *Phys. Lett.* **B 343**, 310 (1995).
- [50] A. M. Badalian *Phys. Atom. Nucl.* **63**, 2173 (2000);  
 A. M. Badalian and D. S. Kuzmenko *Phys. Rev.* **D 65**, 016004 (2001)  
 [hep-ph/0104097];  
 S. G. Gorishnii, A. L. Kataev and S. A. Larin, *Phys. Lett* **B 135**, 457 (1984);  
 A. L. Kataev, *Phys. Atom. Nucl.* **68**, 567 (2005) [hep-ph/0406305].
- [51] S. Godfrey and N. Isgur, *Phys. Rev.* **D 32**, 189 (1988).
- [52] D. Ebert, R. N. Faustov and V. O. Galkin, *Phys. Rev.* **D 79**, 114029 (2009)  
 [arXiv:0903.5183].
- [53] R. Giachetti and E. Sorace, *Phys. Rev.* **D 87**, 034021 (2012)  
 [arXiv:1207.3301].
- [54] F. Verstraete, V. Murg and J. I. Cirac, *Adv. Phys.* **57**, 143 (2008)  
 [arXiv:0907.2796];  
 R.Orus, *Ann. Phys.* **349** 117 (2014) [arXiv:1306.2164].
- [55] A. M. Badalian, private communication.
- [56] A. Badalian, M. Lukashov and Y. A. Simonov, – arXiv:2001.07113.